Available online at www.sciencedirect.com
SCIENCE DIRECT®
Global and Planetary Change 39 (2003) 257–269
GLOBAL AND PLANETARY CHANGE
www.elsevier.com/locate/gloplacha

Paleoclimate implications of high latitude precession-scale mineralogic fluctuations during early Oligocene Antarctic glaciation: the Great Australian Bight record

David J. Mallinson[a,*], Benjamin Flower[b,1], Albert Hine[b,1], Gregg Brooks[c], Roberto Molina Garza[d,2]

[a] *Department of Geology, East Carolina University, 101 Graham Building, Greenville, NC 27858-4353, USA*
[b] *College of Marine Science, University of South Florida, St. Petersburg, FL 33701, USA*
[c] *Department of Marine Science, Eckerd College, St. Petersburg, FL 33705, USA*
[d] *Unidad de Ciencias de la Tierra, Campus Juriquilla UNAM, Juriquilla, Queretaro, Mexico 76230, Mexico*

Abstract

Sediments from ODP Site 1128 in the Great Australian Bight record isotopic and mineralogic variations corresponding to orbital parameters and regional climate change during the early Oligocene climate transition and Oi1 glacial event. Bulk carbonate stable isotope analyses reveal prominent positive oxygen and carbon isotope shifts related to the inferred major increase in glaciation at approximately 33.6 to 33.48 Ma. The oxygen isotope excursion corresponds to a prolonged period of low eccentricity, suggesting ice-sheet growth during low seasonality conditions. The clay mineralogy is dominated by smectite throughout. The exclusive occurrence of highly crystalline smectite from 33.6 to 33.5 Ma suggests the occurrence of explosive volcanism that correlates with the positive oxygen isotope shift. The dominance of mixed-layer smectite from 33.5 to 33.4 Ma and an increase in illite following 33.4 Ma indicates a transition from cool, wet conditions to cool, dry conditions over Australia during the Oi1 glaciation. Clay mineralogy and carbonate percentages reveal precession-scale oscillations during the Oi1 event. Kaolinite varies inversely with smectite and percent carbonate. Variations in precipitation and runoff, and wind velocities during southern hemisphere summer perihelion and high eccentricity intervals may account for the precession-scale oscillations.

Keywords: Precession; Eccentricity; Orbital-forcing; Australian–Antarctic Seaway; Antarctic glaciation; Oligocene; Clay mineralogy; Great Australian Bight

1. Introduction

The early Oligocene marks a significant transition in global climate and provides the first strong evidence of permanent Cenozoic glaciation on Antarctica (Kennett, 1977; Miller et al., 1991; Zachos et al., 1992; Moss and McGowran, 1993; Flower, 1999; Barker et al., 1999). The progressive widening of the Australian–Antarctic Seaway (AAS) and subsidence of the

* Corresponding author. Fax: +1-252-328-4391.
E-mail addresses: mallinsond@mail.ecu.edu (D.J. Mallinson), bflower@seas.marine.usf.edu (B. Flower), ahine@seas.marine.usf.edu (A. Hine), brooksgr@eckerd.edu (G. Brooks), rmolina@unicit.unam.mx (R.M. Garza).
[1] Fax: +1-727-553-1189.
[2] Fax: +52-56234100.

0921-8181/$ - see front matter © 2003 Elsevier B.V. All rights reserved.
doi:10.1016/S0921-8181(03)00119-X

Tasman Rise during the late Eocene contributed to the establishment of surface and deep water circulation, the thermal isolation and cooling of Antarctica, and provided the setting for the expansion of continental glaciation (Kennett, 1977). Various investigations have examined the nature of the early Oligocene climate transition based upon the isotopic record (Miller et al., 1991; Zachos et al., 1992, 1994, 1996), and the sedimentologic and mineralogic records in the Southern Ocean (Ehrmann and Mackensen, 1992; Wise et al., 1992; Robert and Kennett, 1997; Barker et al., 1999) and the paleontologic record (Moss and McGowran, 1993; McGowran et al., 1997). Other investigations have focused on the Neogene record of the Antarctic Ice Sheet (Barker et al., 2002; Hillenbrand and Ehrmann, 2002). However, questions remain regarding the forcing mechanisms for ice-sheet development, and the high frequency record of the climate transition.

Corresponding to the late Eocene to early Oligocene global cooling and ice sheet development on Antarctica, there was also a significant climate transition in Australia (Moss and McGowran, 1993). Palynological data indicate that southern Australian paleoclimate during the middle Eocene was characterized by high annual temperatures (>24 C) and high annual rainfall (>1500 mm) with no marked seasonality (Alley, 1998). During the late Eocene, there was a moderation of temperatures (<20 C) and rainfall (>1000 mm) (Alley, 1998), and during the Oligocene the climate became more savanna-like (Clarke, 1998). Neritic biostratigraphic data also indicate a pronounced cooling episode in Southern Australia during the early Oligocene ("Chill II" during Chron C13n) that correlates with the Oi1 glacial event as described by Zachos et al. (1994, 1996) (McGowran et al., 1997; Chaproniere et al., 1995) and the Chinaman Gully regression (Moss and McGowran, 1993) on the south Australian margin.

This investigation provides a high-resolution record (~3–5-ky sample interval, based upon interpolated magnetostratigraphic data) of the early Oligocene climate transition in the Great Australian Bight, an area affected by Southern Ocean circulation as well as eolian and fluvial input from Australia. Furthermore,

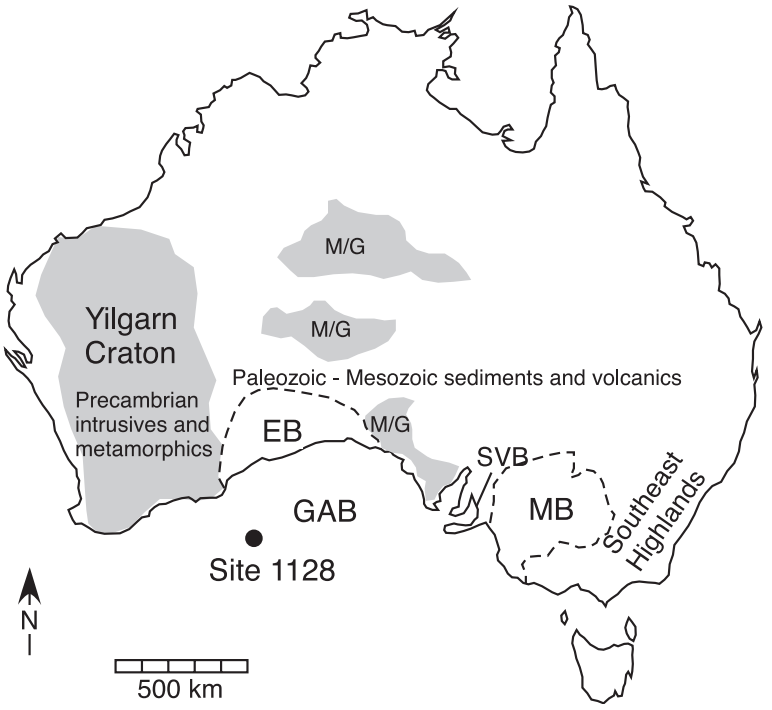

Fig. 1. Map showing the location of ODP Leg 182, Site 1128B within the Great Australian Bight (GAB), and geologic terranes referred to in the text. EB=Eucla Basin; SVB=St. Vincent Basin; MB=Murray Basin; M/G=High grade metamorphics and associated granites.

data are compared to orbital parameters (Shackleton et al., 1999) in order to evaluate the role of orbital geometry in the establishment of perhaps the first significant glacial of the Cenozoic.

Site 1128 is the deep-water site for Leg 182 in the Great Australian Bight (Fig. 1). This site is located on the upper continental rise in 3874 m of water, and is approximately 200 km south of the Australian mainland (Feary et al., 2000). The paleolatitude of this site during the early Oligocene was approximately 52°S placing it approximately 1500 km from Antarctica. Given a depth below seafloor of ~240 m, and a current water depth of 3874 m, and assuming typical thermal subsidence, the paleo-water depth of this site at 33 Ma was approximately 2100 m. Early Oligocene sediments at site 1128 are hemipelagic, clayey, diatomaceous, spiculitic, nannofossil oozes.

Factors that influence clay formation include temperature, precipitation, and parent material (Birkeland, 1984). Clay minerals in marine sediments are the result of weathering and diagenetic conditions in the source terranes, and in the depositional environment (Moore and Reynolds, 1997) and, as such, can provide a record of the changing sources and transporting agents, and regional climate variability over long time periods (10^6 years) occurring in response to the widening of the AAS and Antarctic glaciation. The relationship of the clay mineralogy at Site 1128 to other parameters, such as carbonate percentages and isotopic data, provides a view of the Great Australian Bight regional climate response to the onset of early Oligocene glaciation.

2. Methods

Preparation for X-ray diffraction analyses included separation of the <2-μm size fraction from bulk samples by sieving and centrifuging. Bulk samples were disaggregated in an ultrasonic bath and wet-sieved to separate the >63-μm size fraction from the mud fraction. The silt size fraction was isolated by centrifuging the sample suspension at 1000 rpm for 2.5 min. The <2-μm size fraction that remained in suspension was decanted and centrifuged at 10,000 rpm for 10 min to concentrate the clay fraction. The <2 μm size fraction was distributed on a glass slide as a slurry, and allowed to air-dry to produce a texturally oriented clay film. Clay samples were ethylene glycol solvated for ~24 h immediately before mineralogic analysis. Mineralogic analyses were performed at the College of Marine Science-University of South Florida using a Scintag XDS 2000 X-ray diffractometer with CuKα radiation (40 kV, 35 mA) on oriented and glycolated clays. The clay size fraction was scanned from 2° to 40° 2è at a scan rate of 0.02°/s. Clay mineralogy was assessed according to methods outlined in Moore and Reynolds (1997). The main clay mineral groups were identified by their basal reflections at ~17 Å (ethylene glycol solvated smectite), 10 and 5 Å (illite), and 7 and 3.57 Å (kaolinite). No chlorite (14.2 Å) was detected in these samples. Percent interlayered illite within mixed-layer illite–smectite was determined using the method of Moore and Reynolds (1997). Clay mineral abundance was evaluated semi-quantitatively by determining the area under the 001 peak on XRD records, using the DMS software peak-fitting function. Peak areas were summed for all detected clay minerals (illite, smectite, kaolinite) present within a sample, then each peak area was divided by the sum to arrive at a peak area ratio. The peak area ratio provides a useful tool for determining relative clay mineralogic variations downcore, particularly when presented as relative indices of kaolinite/smectite, smectite/illite, and kaolinite/illite (Robert and Kennett, 1997).

Standard sedimentological procedures were used for grain size analyses. Grain size was determined for the coarse (<4 ϕ;>63 μm) fraction using the settling tube method (Gibbs, 1974) and for the fine (>4 ϕ;<63 μm) fraction using the pipette method (Folk, 1965). Total carbonate was measured on bulk samples using acid digestion and filtration methods. Color reflectance measurements were collected aboard the D/V JOIDES Resolution during Leg 182 (Feary et al., 2000).

Carbon and oxygen isotopic investigations of bulk carbonate samples were performed at the College of Marine Science-University of South Florida using a Finnigan/MAT DeltaPlus XL isotope ratio mass spectrometer equipped with a Kiel III automated carbonate preparation device. Bulk sediment samples were first baked in vacuo at 375 °C for 1 h to deactivate organic carbon prior to acid digestion. All measurements are reported as per mil relative the VPDB carbonate standard. External precision based on over 400 NBS-19 standard run since July 2000 is ±0.04 for $\delta^{13}C$ and ±0.06 for $\delta^{18}O$.

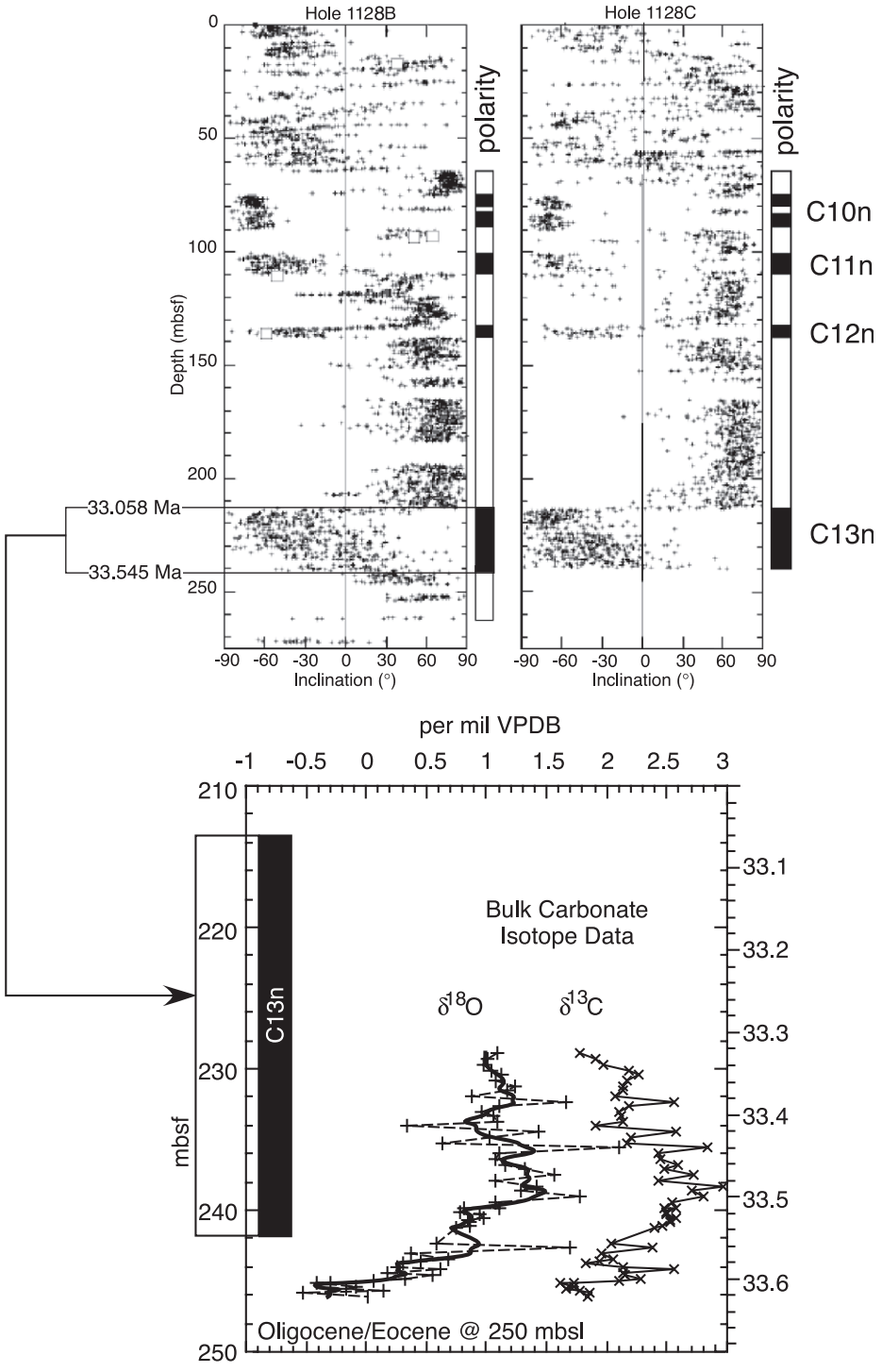

Fig. 2. Magnetostratigraphic data from Site 1128 (Feary et al., 2000), bulk carbonate isotopic data presented in relation to meters below seafloor, the position of Chron 13n, and the corresponding age. The age model used in this manuscript is linearly interpolated between the upper and lower boundaries of C13n, and linearly extrapolated below C13n. Oxygen isotope data are presented showing all data points and as a smoothed curve.

3. Results

3.1. Age model

Mineralogic and isotopic data are presented in Figs. 2–5. Biostratigraphic data confirm an early Oligocene age for these sediments, but are poorly constrained in this section (Feary et al., 2000). Our age model is based upon the geomagnetic polarity time scale of Berggren et al. (1995) and is constrained by the occurrence of the base of Chron 13n (33.545 Ma) at 241.8±1 mbsf in Site 1128B, and the top of C13n (33.058 Ma) at 213.5±0.2 mbsf in Site 1128B and 1128C (Feary et al., 2000) (Fig. 2). Sample ages were linearly interpolated between these two horizons, assuming constant sedimentation over this ~500-ky interval. The ±1-m uncertainty in the position of the lower chron boundary results in a thickness uncertainty for C13n of ±4%. The 28.3-m thickness of C13n yields a corresponding age uncertainty of approximately ±19.5 ky. Other studies have shown that uncertainties in the duration of individual chrons determined by analyses of marine magnetic anomalies and a set of distributed calibration points are also in the order of a few percent (Cande and Kent, 1995; Huestis and Acton, 1997). The resulting accumulation rate is 58.1 m/my, and agrees well with accumulation rates estimated from the biostratigraphic data for this interval (50–60 m/my; Feary et al., 2000) Samples were taken at 20-cm intervals yielding an inferred age resolution of approximately 3000 years.

Bulk carbonate isotopic data support the absolute age assigned to the section as well as the age model as defined by the magnetostratigraphy. Isotope data reveal a well-defined +2‰ $\delta^{18}O$ shift, with a steep gradient between 246 and 239 mbsl (33.6 to 33.5 Ma based on our age model) (Fig. 2). Peak $\delta^{18}O$ values occur between 239 and 237 mbsl (33.52 to 33.48 Ma) and correlate with the Oi-1a $\delta^{18}O$ shift as defined by Zachos et al. (1996), which exhibits peak $\delta^{18}O$ values at ~33.52–33.48 Ma at ODP Sites 774 and 522. Based on the correlation of the bulk carbonate $\delta^{18}O$ peak to the data of Zachos et al. (1996), the estimated age uncertainty is approximately ±20 ky; the same as indicated by the magnetostratigraphic data. The $\delta^{13}C$ shift is less well defined, but occurs in several steps that coincide with the $\delta^{18}O$ shift (Fig. 2).

3.2. Mineralogy

Clay minerals throughout the sedimentary column at Site 1128 are dominated by smectite with varying amounts of illite interlayers (Fig. 3). On average, kaolinite is the second most abundant clay mineral (in terms of peak area ratio), followed by discrete illite. The clay mineralogic record between 33.7 and 33.5 Ma consists exclusively of highly crystalline smectite with <10% mixed-layers, except for a very minor fraction of kaolinite at 33.6 Ma (Fig. 3). At 33.5 Ma, there is a sudden appearance and rapid increase of kaolinite and illite, and mixed-layer illite–smectite (10–30% illite interlayers) (Fig. 3). Between 33.44 and 33.24 Ma, there are nine peaks in the kaolinite/smectite index, indicating a periodicity of ~22 ky (Fig. 4).

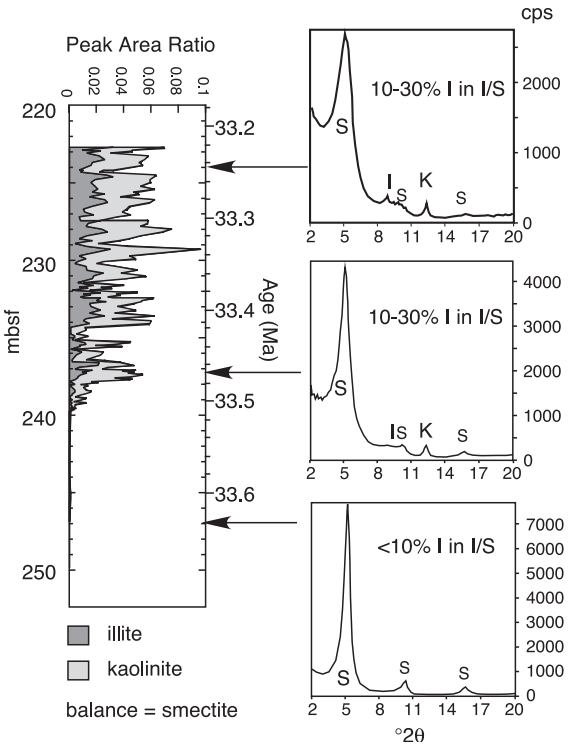

Fig. 3. Clay mineral abundance expressed as peak area ratio (see text for discussion), with diffractograms illustrating the upward increase in kaolinite (K) and illite (I) through the section, and the dominance of smectite (S) throughout. Note that the Peak Area Ratio scale maximum is 0.1 out of a possible 1.0. Also, note the different vertical scales in the three diffractograms. %I refers to the percentage of illite interlayers within smectite (S).

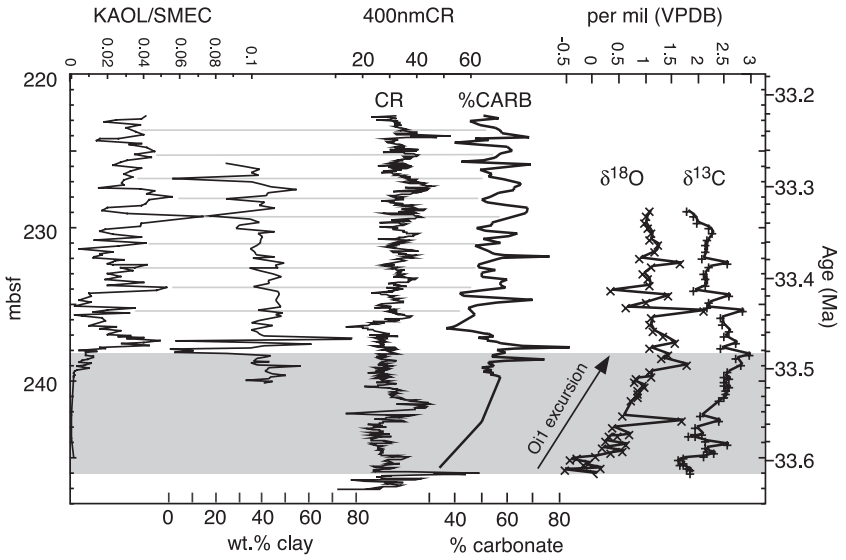

Fig. 4. Isotopic and mineralogic data from the Eocene/Oligocene boundary at Site 1128B. Data shown (from top down) include carbon and oxygen isotopes from bulk carbonate samples, wt.% carbonate, 400 nm color reflectance (CR), wt.% clay, and the kaolinite/smectite index. Correlation lines are added to illustrate the relationship between the kaolinite/smectite index, wt.% clay, and wt.% carbonate. Depth units are in meters below seafloor.

Greatest variance within the clay mineralogy is controlled by fluctuations in smectite and kaolinite, which exhibit a strong negative correlation (r^2= −0.89). Smectite versus illite exhibits a somewhat weaker negative correlation (r^2=−0.73). Finally, kaolinite versus illite exhibits no significant correlation (r^2=0.4).

The early Oligocene record at Site 1128 reveals initially high carbonate percentages corresponding to a 20-m-thick nannofossil chalk unit (Hine et al., 1999; Feary et al., 2000; Mallinson et al., 2003). This interval of high carbonate abundance occurs during Chron 13 n. The carbonate fraction at this deep-water site is exclusively low-Mg calcite derived from nannofossils. Carbonate percentages range from 34% to 84%. Carbonate percentages increase from a mean of approximately 35% to approximately 55% across the Eocene/Oligocene boundary (Feary et al., 2000; Swart et al., 2002; Mallinson et al., 2003) then oscillate between approximately 45% and 70% with a periodicity of approximately 22 ky (Fig. 4). In most instances, wt.% carbonate appears to vary inversely to the kaolinite/smectite index. The 400-nm color reflectance record approximately mimics the percent carbonate.

4. Discussion

4.1. Isotopic and mineralogic interpretations

The +2‰ δ^{18}O shift recorded in bulk carbonate samples (Fig. 2) correlates with the Oi1 shift defined by Miller et al. (1991), which is inferred to correspond to a major increase in continental glaciation on Antarctica (Zachos et al., 1992, 1996). Based upon our age model, the Oi1 shift is defined between 33.6 and 33.48 Ma; 33.6 Ma is a minimum age as no isotopic analyses were performed on earlier samples. The positive δ^{18}O shift is synchronous with the increase in carbonate accumulation (Fig. 4), which may reflect a deepening CCD, resulting from surface water cooling, glacial increase, and deep-water ventilation. Increased ventilation at this time is also indicated by faunal and sedimentologic changes in the St. Vincent Basin to the east (Moss and McGowran, 1993). The positive δ^{13}C shift is recognized as a global phenomenon, and has been attributed to a global increase in organic carbon burial in response to increased oceanic turnover and upwelling (Shackleton and Kennett, 1975; Moore et al., 1978), and increased carbonate and biogenic silica accumulation rates (Zachos et al., 1996). A

decrease in natural gamma values and magnetic susceptibility in the early Oligocene at Site 1128 reflects dilution of the terrigenous component by increased carbonate accumulation (Mallinson et al., 2003).

The clays occurring at Site 1128 suggest multiple origins and sources with a wide range of precipitation and temperature characteristics. The proximity of Site 1128 to Australia and the general wind patterns modeled during the Eocene (Sloan and Huber, 2001) suggest that Australia was the dominant source for the clays (both fluvial and eolian transported). Robert and Kennett (1997) identified contemporaneous clay mineral assemblages derived from Antarctica (Maud Rise; Site 689) consisting of significant smectite and kaolinite, but also containing significantly more illite and chlorite than our samples. Hillenbrand and Ehrmann (2002) evaluated Miocene through Quaternary clay mineral assemblages dominated by smectite, illite and chlorite, with traces of kaolinite, from the continental margin west of the Antarctic Peninsula (ODP Leg 178). The general lack of chlorite and the low abundance of illite in our samples support Australia as the dominant source.

Smectite may form by continental weathering in soil profiles, producing mixed-layer varieties (detrital smectite), or by alteration of volcanic glass, resulting in smectite with <10% interlayers (authigenic smectite) (Jones and Fitzgerald, 1984; Compton et al., 1992; Hillenbrand and Ehrmann, 2002). Detrital smectite is the most abundant and widespread clay mineral in sedimentary rocks and soils and can form under a variety of conditions, but generally occurs as a weathering product of mafic to felsic rocks under conditions of cool temperatures and moderate precipitation, producing moderate rates of chemical weathering (Birkeland, 1984; Moore and Reynolds, 1997; Robert and Kennett, 1997). The occurrence of kaolinite indicates a source with high precipitation and warm soil temperatures (minimum of 15 °C; Gaucher, 1981), yielding intense leaching and high rates of chemical weathering (Birkeland, 1984; Chamley, 1989). Illite may be representative of colder, more arid climates, dominated by physical weathering, but also may be derived from alteration of biotite under warmer and wetter conditions (Birkeland, 1984).

The clays were likely derived from erosion of terranes in the southwest and the central interior of Australia in the vicinity of the Eucla Basin, and the Yilgarn Craton (Fig. 1). The Yilgarn Craton is northwest of Site 1128, and consists of deeply weathered Precambrian felsic to intermediate intrusives and metamorphic terranes comprised of significant kaolinite-rich soils (Palfreyman, 1984; Anand, 1998; Clarke, 1998). Gingele et al. (2001) indicate that the Yilgarn Craton is a major source of kaolinite, and minor source of illite, to the coastal and marine system of western Australia via fluvial and eolian transport. The Australian interior (the Great Victorian Desert) east of the Yilgarn Craton exhibits a dramatic decrease in precipitation relative to the Yilgarn Craton. The interior also provides deeply weathered volcanics and sediments that, combined with moderate, seasonal rainfall, provided ideal conditions for the formation of detrital smectite. Although the climate of this area is currently arid, there are significant paleodrainage systems within the Eucla Basin, most notably, the Lefroy paleodrainage channel and the Cowan paleodrainage channel (Alley, 1998). These channels are major paleofluvial valleys that were active during the Eocene and early Oligocene and are incised to depths of 200 m, and are 15–40 km in width (Clarke, 1998). Clays were likely transported to the vicinity of Site 1128 by a combination of fluvial, eolian, and shelf currents.

4.2. Long-term variations

An interval of authigenic smectite occurs below 240 mbsl (approximately 33.7 to 33.5 Ma) (Figs. 3–5), coincident with the Oi1 isotope shift. The authigenic smectite may have been derived from alteration of volcanic ash and presents the possibility of regional explosive volcanism that coincided with the Oi1 isotope shift. Highly smectitic sediments are also present in the late Eocene to early Oligocene Blanche Point Formation in the St. Vincent Basin of South Australia (Fig. 1). The top of the Blanche Point Formation is an unconformable surface that correlates with the base of C13n (McGowran and Li, 1998). The origin of the silicified Blanche Point deposits has been attributed to alteration of ash from explosive volcanism associated with the final stages of separation of Australia from Antarctica (Jones and Fitzgerald, 1984). The site of explosive volcanism is not clear. Jones and Fitzgerald (1984) suggest a trailing edge site; however, prevailing winds in this area were likely out of the northwest during the Eocene (Sloan and Huber, 2001) and may

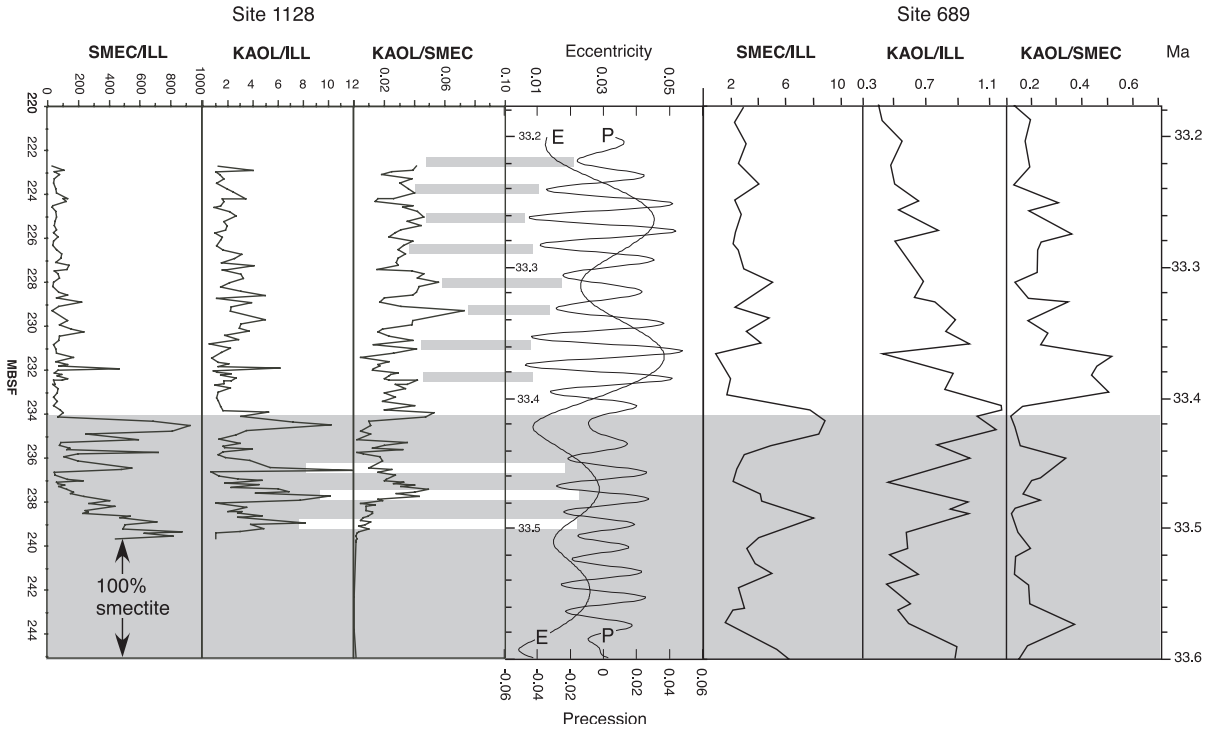

Fig. 5. Clay mineral indices from Site 1128 (this investigation), and Site 689 (Robert and Kennett, 1997). Illite is much more abundant at Site 689 owing to the proximity to Antarctica. Also shown are precession (P) and eccentricity (E). Southern hemisphere summer perihelion orbits are represented by southern hemisphere precession maxima (negative values). The kaolinite/smectite cycles are of the same periodicity as precession; however, a precise correlation cannot be made due to the age uncertainty of ±20 ky. Note the correspondence of high smectite/illite and kaolinite/illite values with the period of low eccentricity (shaded, below 234 m; 33.42 Ma). Also highlighted are three peaks of apparent precession periodicity (white bars) within the kaolinite/illite index between 33.45 and 33.5 Ma.

have delivered ash from the leading edge of the Australian Plate.

The smectite occurring above 240 mbsl (<33.5 Ma) is the mixed-layer variety, consisting of 10–30% interlayed illite (detrital smectite). The appearance of detrital smectite, kaolinite, and discrete illite at 33.5 Ma (Figs. 3 and 4) indicates a change in the style of weathering and clay formation in the region, or a change in clay mineral source. A change in the clay mineral source could result from a decrease in volcanic ash input, a change in the dominant transporting agent (fluvial or eolian), a shift in the dominant fluvial point source and corresponding drainage basin and provenance, or a combination of these factors.

A prolonged period of low eccentricity occurred from 33.6 to 33.4 Ma (Shackleton et al., 1999). The combination of low eccentricity and low obliquity reduces seasonality and is considered conducive to ice-sheet development (Zachos et al., 2001), and may have been the major factor in ice-sheet growth at this time. Reduced seasonality produces cooler summers, warmer winters, higher precipitation rates, and reduced winds (Veevers, 1984; Trenberth, 1993; Sloan and Huber, 2001). The largest peaks in the smectite/illite ratio at 33.50 and 33.42 Ma occur during the period of minimal eccentricity (Fig. 5). Dominance of detrital smectite (above the zone of authigenic smectite) during the low eccentricity period until 33.42 Ma is consistent with wet and cool conditions on Australia.

Fluctuations in clay mineralogy during the early Oligocene also were noted from Site 689, Maud Rise, Antarctica (Robert and Kennett, 1997), and related to climate cooling, a transition from chemical to physical weathering on Antarctica, and development of the cryosphere. It is difficult to compare our data (Site 1128) directly to Robert and Kennett's (1997) as our

data are at a higher temporal resolution, and the study locations are on opposite sides of Antarctica. However, similarities between the records do exist (Fig. 5). Site 1128 and Site 689 both reveal a peak in the smectite/illite index at ~33.5 and 33.4 Ma, suggesting an increase in chemical weathering resulting from high precipitation rates at high latitude. Higher annual precipitation combined with cooler summers at high southern latitudes may have also contributed greatly to the rapid growth of the Antarctic ice sheet at this time (Robert and Kennett, 1997).

Following 33.42 Ma, Site 1128 exhibits a permanent increase in illite relative to kaolinite and smectite (Figs. 5 and 6), although detrital smectite remains the dominant clay mineral. This mineralogic transition corresponds to the onset of high eccentricity conditions at 33.42 Ma, and maximum $\delta^{18}O$ values of bulk carbonate at Site 1128, and suggests a general decrease in weathering corresponding to cooler, drier conditions in the Australian continental interior. Alternatively, the increase in illite could simply indicate the exposure of a fresh source of illitic clays (e.g., mica-rich metamorphic terranes). Concurrently, the cyclicity in the kaolinite/smectite index at Site 1128 indicates that the weathering and delivery of clays from existing lateritic terranes in Southern Australia remained significant.

4.3. Short-term variations

It is significant, but not unexpected, that precession periodicity exists at this fairly high latitude (paleolatitude of ~52°S). Sloan and Huber (2001) found that sea-surface temperatures at high latitudes were highly sensitive to precession-driven changes in insolation during the Paleogene. Kroon et al. (1999) describe precession–length cycles from middle Eocene sediments in the western Atlantic, and relate them to variations in upwelling processes. Precessional signals have also been defined in other Paleogene records (Fischer and Roberts, 1991; Roehler, 1993). The occurrence of a precession signal is likely a response to the increase in eccentricity at ~33.4 Ma, as eccentricity modulates the magnitude of the precession effect (Bradley, 1999).

The complex variability of the early Oligocene clay mineralogy at Site 1128 indicates precession-scale changes in wind characteristics, or precipitation and runoff that affected clay sources or transport agents.

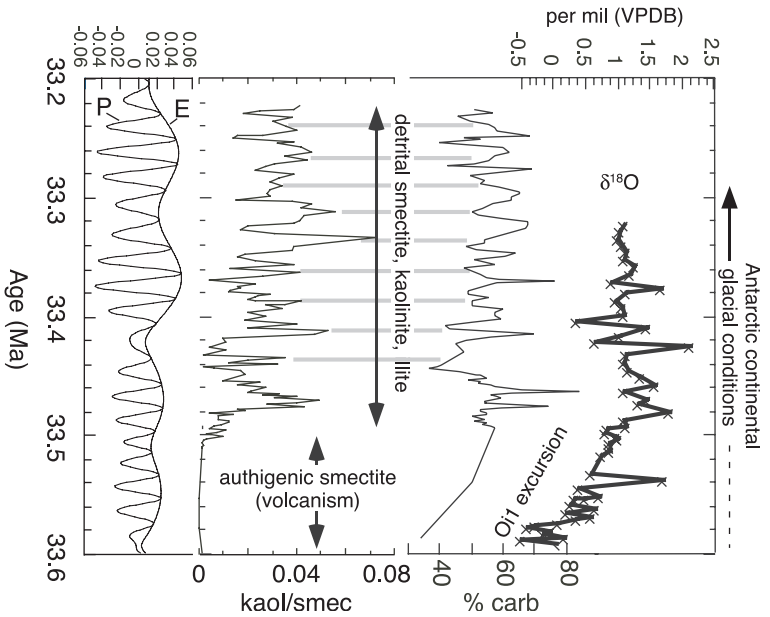

Fig. 6. Relationship of the Oi1 isotope excursion to wt. % carbonate, kaolinite/smectite index, clay facies, and eccentricity (E) and precession (P) (Shackleton et al., 1999). Ages are based on the time-scale of Berggren et al. (1995).

The variations occur too rapidly to reflect changes in weathering rates in the source areas (Birkeland, 1984; Thiry, 2000; Gingele et al., 2001). First of all, there is a clear transition at approximately 33.42 Ma (231 mbsf) in the cyclic occurrence of the clay minerals. Prior to 33.42 Ma there is a strong precessional component in the kaolinite/illite index (Fig. 5). Following ~33.42 Ma, cyclicity in the kaolinite/illite index terminates, and is replaced by strong cyclicity in the kaolinite/smectite index. This transition correlates very well with the transition from low to high eccentricity (Fig. 5), and suggests that an increase in seasonality affected the mode of clay transport.

The simplest mechanism to explain the high frequency (~22 ky) variations calls on precession-driven variations in wind patterns and precipitation and runoff, and a corresponding change in the flux and mineralogy of the clays being delivered to the Eucla Basin and Great Australian Bight by fluvial and eolian processes. Sloan and Huber (2001) modeled the latitudinal temperature response to orbital forcing during the Paleogene. Their MINS model, which corresponds to southern hemisphere precession maxima (summer perihelion orbits; warmer summers, cooler winters; increased seasonality), suggests that high-latitude (southern hemisphere) low-pressure systems and subtropical highs intensify during December through February, resulting in greater wind velocities, particularly along the coast of Antarctica. Warmer summers associated with periods of increased seasonality would likely have corresponded to a decrease in precipitation rates in the continental interior (Veevers, 1984; Trenberth, 1993; Sloan and Huber, 2001), a decrease in clay flux to the coastal system, and reduced vegetative cover, resulting in increased wind erosion of the deeply weathered, kaolinite-rich, lateritic residuum of the Yilgarn Craton (Anand, 1998). Concurrently, strengthened pressure cells and increased meridional pressure gradients during southern hemisphere precession maxima should increase wind velocities, causing greater upwelling along the polar front (Sloan and Huber, 2001), increased siliceous productivity, a shoaling lysocline, and a decrease in carbonate accumulation, resulting in an inverse relationship between kaolinite and carbonate.

During southern hemisphere precession minima (winter perihelion orbits; cooler summers, warmer winters; decreased seasonality), summer temperatures and wind velocities decrease as the Australian low pressure cell weakens, and chemical weathering may be slightly reduced due to cooler summer temperatures. The increased precipitation and resulting increased vegetative cover, combined with decreased wind velocities, would decrease eolian flux of kaolinite to the GAB, but would increase fluvial transport of clays. Fluvial delivery of dominantly smectitic clay minerals from weathered volcanics to the GAB area would have been easily facilitated through the extensive paleodrainage systems feeding the Eucla Basin (Alley, 1998; Clarke, 1998). In the marine environment, weakened pressure cells would have decreased wind flow and upwelling, resulting in a deepening lysocline and greater carbonate preservation. This scenario satisfies all of the observed relationships between the various data sets (Fig. 4).

The Leeuwin Current may have acted as an additional transporting agent for kaolinite from areas draining the Yilgarn Craton to the west. The Leeuwin Current is a shallow, warm-water current that runs southward along the coast of Western Australia and into the Great Australian Bight (Smith et al., 1991; Gingele et al., 2001), and is presently a major factor in transporting kaolinite along the Western Australian coastline (Gingele et al., 2001). However, the current typically shuts down during cold periods (glacials) as the subtropical convergence zone and Polar Front are deflected northward (McGowran et al., 1997). Variations in the kaolinite content of the sediments at Site 1128 might then indicate fluctuations in the flow of a paleo-Leeuwin Current, perhaps in response to the position of the subtropical convergence zone and Polar Front.

An alternate mechanism could include a change in the prevailing wind direction that may have shifted the source terrane for clays in our samples. A shift in the prevailing wind direction is expected to accompany a change in meridional pressure gradients corresponding to strengthening and weakening pressure cells, in response to insolation changes (Sloan and Huber, 2001). The location of Site 1128 during the early Oligocene places it close to the polar front, an area where the polar easterlies and the westerlies converge. A small expansion or contraction of the front could place the site under the influence of either northwest winds or southeast winds. The former wind direction would transport dominantly smectitic and

kaolinitic clays from Australia, whereas the latter direction would transport larger amounts of illite from Antarctica. It is possible that this mechanism explains the precession-scale variations in the kaolinite/illite index between 33.5 and 33.42 Ma. However, the absence of chlorite in our samples argues against significant influx from Antarctica. Also, this scenario would likely result in a greater negative correlation between kaolinite and illite, and a positive correlation between smectite and kaolinite, neither of which are observed.

5. Summary

The early Oligocene record (Chron 13n) at ODP Site 1128 in the Great Australian Bight reveals mineralogic variations that are related to changes in temperature and precipitation over southern Australia, driven by variations in eccentricity and precession. The nature of the suggests that ice-sheet expansion on Antarctica may have been initiated by a prolonged period of low eccentricity, similar to the Mi1 event during the Miocene (Zachos et al., 2001). From at least 33.7 to 33.5 Ma, authigenic smectite is the sole clay mineral, suggesting a volcanic ash origin. From 33.5 to 33.4 Ma, detrital smectite (10–30% illite interlayers) occurs with minor amounts of kaolinite and discrete illite. The correlation of detrital smectite with low eccentricity suggests the existence of cool conditions over Australia, with moderate amounts of rainfall accompanying reduced seasonality at high southern latitudes. The increase in kaolinite and illite at 33.4 Ma correlates to high eccentricity conditions and is inferred to correspond to increased physical weathering, increased winds, dryer conditions, and increased eolian transport of clays from the deeply weathered regolith of the Yilgarn and Western Cratons. Precession-scale variations also occur in mineralogic factors in the GAB, most likely in response to changes in seasonality that affected precipitation patterns, runoff, vegetative cover, and wind intensity over southern Australia.

Acknowledgements

The authors would like to acknowledge the contributions of the co-chief scientist, David Feary, staff scientist Mitchell Malone, the ODP Leg 182 Shipboard Scientific Party, and the captain and crew of the D/V JOIDES Resolution. This paper benefited from the constructive reviews of S. Hovan and A. Cooper. This investigation was supported with funding from the US Science Support Program and the Texas A&M Research Foundation.

References

Alley, N.F., 1998. Evidence of early Tertiary palaeoclimate from the Eucla Basin palaeodrainage area: the State of the Regolith. Geological Society of Australia Special Publication 20, 104–109.

Anand, R.R., 1998. Distribution, classification and evolution of ferruginous materials over greenstones on the Yilgarn Craton—implication for mineral exploration: the State of the Regolith. Special Publication-Geological Society of Australia 20, 175–193.

Barker, P.F., Camerlenghi, A., Acton, G., Ramsay, A.T., the Leg 178 Shipboard Scientific Party, 2002. Proceedings of the Ocean Drilling Program, vol. 178. Scientific Results, Antarctic Glacial History and Sea-level Change. 33 pp.

Barker, P.F., Barrett, P.J., Cooper, A.K., Huybrecht, P., 1999. Antarctic glacial history from numerical models and continental margin sediments. Palaeogeography, Palaeoclimatology, Palaeoecology 150, 247–267.

Berggren, W.A., Kent, D.V., Swisher III, C.C., Aubry, M.-P., 1995. A revised Cenozoic geochronology and chronostratigraphy. In: Berggren, W.A., Kent, D.V., Aubry, M.-P., Hardenbol, J. (Eds.), Chronology, Time Scales and Global Stratigraphic Correlation. SEPM Special Publication, vol. 54. 386 pp.

Birkeland, P.W., 1984. Soils and Geomorphology. Oxford Univ. Press, New York. 372 pp.

Bradley, R.S., 1999. Paleoclimatology. Academic Press, San Diego. 613 pp.

Cande, S.C., Kent, D.V., 1995. A revised calibration of the new geomagnetic polarity time scale for the late Cretaceous and Cenozoic. Journal of Geophysical Research 100, 6093–6095.

Chamley, H., 1989. Clay Sedimentology. Springer-Verlag, Berlin. 623 pp.

Chaproniere, G.C., Shafik, S., Truswell, E.M., Macphail, M.K., Partridge, A.D., 1995. Cainozoic. Australian Phanerozoic Time Scales, vol. 10. Australian Geological Survey Organization, Record, Canberra.

Clarke, J.D.A., 1998. Ancient landforms of Kambalda and Norseman: the state of the Regolith. Geological Society of Australia Special Publication 20, 40–49.

Compton, J.S., Mallinson, D., Netratanawong, T., Locker, S., 1992. Regional correlation of mineralogy and diagenesis of sediment from the Exmouth Plateau and Argo Basin, Northwestern Australian Continental Margin. In: Gradstein, F.M., Ludden, J.N. (Eds.), Proceedings of the Ocean Drilling Program. Scientific Results, vol. 123, pp. 779–790.

Ehrmann, W.U., Mackensen, A., 1992. Sedimentological evidence for the formation of an east Antarctic ice sheet in Eocene/Oligocene time. Palaeogeography, Palaeoclimatology, Palaeoecology 93, 85–112.

Feary, D.A., Hine, A.C., Malone, M.J., et al., 2000. Proceedings of the Ocean Drilling Program. Initial Reports 182. College Station, TX, 52 pp.

Fischer, A.G., Roberts, L.T., 1991. Cyclicity in the Green River Formation (lacustrine Eocene) of Wyoming. Journal of Sedimentary Petrology 61, 1146–1154.

Flower, B.P., 1999. Cenozoic Deep-Sea Temperatures and Polar Glaciation: the Oxygen Isotope Record. Terra Antarctica Reports 3, 27–42.

Folk, R.L., 1965. Petrology of Sedimentary Rocks. Hemphill Publ., Austin, TX.

Gaucher, G., 1981. Les facteurs de la pédogenese. G. Lelotte, Dison, Belgium, 730 pp.

Gingele, F.X., Deckker, P.D., Hillenbrand, C.-D., 2001. Clay mineral distribution in surface sediments between Indonesia and NW Australia—source and transport by ocean currents. Marine Geology 179, 135–146.

Gibbs, R.J., 1974. A settling tube for sand-size analysis. Journal of Sedimentary Petrology 44, 583–588.

Hillenbrand, C.-D., Ehrmann, W., 2002. Distribution of clay minerals in drift sediments on the continental rise west of the Antarctic Peninsula, ODP Leg 178, Sites 1095 and 1096. In: Barker, P.F., Camerlaenghi, A., Acton, G.D., Ramsay, A.T.S. (Eds.), Proceedings of the Ocean Drilling Program. Scientific Results 178, pp. 1–29.

Hine, A.C., Feary, D.A., Malone, M.J., Leg 182 Scientific Party, 1999. Research in Great Australian bight yields exciting early results. Eos 80, 525–526.

Huestis, S.P., Acton, G.D., 1997. On the construction of geomagnetic time scales from non-prejudicial treatment of magnetic anomaly data from multiple ridges. Geophysical Journal International 129, 176–182.

Jones, J.B., Fitzgerald, M.J., 1984. Extensive volcanism associated with the separation of Australia and Antarctica. Science 226, 346–348.

Kennett, J.P., 1977. Cenozoic evolution of Antarctic glaciation, the circum-Antarctic Ocean, and their impact on global paleoceanography. Journal of Geophysical Research 82, 3843–3859.

Kroon, D., Norris, R., Kraus, A., ODP Leg 171B Scientific Party, 1999. Variability of extreme Cretaceous–Paleogene climates: evidence from Blake Nose (ODP Leg171B). In: Abrantes, F., Mix, A. (Eds.), Reconstructing Ocean History: A Window into the Future. Kluwer Academic Publishing, Norwell, MA, pp. 295–320.

Mallinson, D.J., Flower, B., Hine, A., Brooks, G.R., Garza, R.M., Drexler, T., and the Leg 182 Shipboard Scientific Party, 2003. Data report: Mineralogy and Geochemistry of ODP Site 1128, Great Australian Bight. In: Hine, A.C., Feary, D.A., Malone, M.J. (Eds.), Proc. ODP, Sci. Results, 182 [Online]. Available from World Wide Web: http://www-odp.tamu.edu/publications/182_SR/001/001.htm.

McGowran, B., Li, Q., 1998. Cainozoic climatic change and its implications for understanding the Australian regolith: the State of the Regolith. Special Publication-Geological Society of Australia 20, 86–103.

McGowran, B., Li, Q., Moss, G., 1997. The Cenozoic neritic record in southern Australia: the biogeohistorical framework. In: James, N.P., Clarke, J. (Eds.), Cool-Water Carbonates. SEPM Special Publication, vol. 56, pp. 185–203.

Miller, K.G., Wright, J.D., Fairbanks, R.G., 1991. Unlocking the ice house: Oligocene–Miocene oxygen isotopes, eustasy, and margin erosion. Journal of Geophysical Research 96, 6829–6848.

Moore, D.M., Reynolds, R.C., 1997. X-ray Diffraction and the Identification and Analysis of Clay Minerals. Oxford Univ. Press, Oxford. 378 pp.

Moore, T.C., Van Andel, T.H., Sancetta, C., Pisias, N.G., 1978. Cenozoic hiatuses in pelagic sediments. Micropaleontology 24, 113–138.

Moss, G., McGowran, B., 1993. Foraminiferal turnover in neritic environments: the end-Eocene and mid-Oligocene events in southern Australia. Memoir of the Association of Australasian Palaeontologists 15, 407–416.

Palfreyman, W.D., 1984. Guide to the geology of Australia. Bureau of Mineral Resources, Bulletin 181 (111 pp.).

Robert, C., Kennett, J.P., 1997. Antarctic continental weathering changes during Eocene–Oligocene cryosphere expansion: clay mineral and oxygen isotope evidence. Geology 25, 587–590.

Roehler, H.W., 1993. Eocene climates, depositional environments, and geography, greater Green River Basin, Wyoming, Utah, and Colorado. U.S. Geological Survey Professional Paper 1506-F.

Shackleton, N.J., Kennett, J.P., 1975. Paleotemperature history of the Cenozoic and the initiation of Antarctic glaciation, oxygen and carbon isotope analyses in DSDP Sites 277, 279, and 281. Initial Reports of the Deep Sea Drilling Project 29, 743–755.

Shackleton, N.J., Crowhurst, S.J., Weedon, G.P., Laskar, J., 1999. Astronomical calibration of Oligocene–Miocene time. Philosophical Transactions of the Royal Society of London 357, 1907–1929.

Sloan, L.C., Huber, M., 2001. Eocene oceanic responses to orbital forcing on precessional time scales. Paleoceanography 16, 101–111.

Smith, R.L., Huyer, A.H., Godfrey, J.S., Church, J.A., 1991. The Leeuwin Current off Western Australia. Journal of Physical Oceanography 21, 322–345.

Swart, P., James, N., Mallinson, D., Malone, M., Matsuda, H., Simo, J., 2002. Data report: the carbonate mineralogy of sites drilled during Leg 182. Proceedings of the Ocean Drilling Program. Scientific Results 182 College Station, TX. Ocean Drilling Program.

Thiry, M., 2000. Palaeoclimatic interpretation of clay minerals in marine deposits: an outlook from the continental origin. Earth Science Review 49, 201–221.

Trenberth, K.E., 1993. Climate System Modeling. Cambridge Univ. Press. 788 pp.

Veevers, J.J., 1984. Phanerozoic Earth History of Australia: Oxford Geological Science Series No. 2. Clarendon Press, Oxford. 418 pp.

Wise Jr., S.W., Breza, J.R., Harwood, D.M., Zachos, J.C., 1992. Paleogene glacial history of Antarctica in light of Leg 120 drilling results. Proceedings of the Ocean Drilling Program. Scientific Results 120, 1001–1030.

Zachos, J.C., Breza, J., Wise, S.W., 1992. Early Oligocene ice-sheet expansion on Antarctica; sedimentological and isotopic evidence from Kerguelen Plateau. Geology 20, 569–573.

Zachos, J.C., Stott, L.D., Lohmann, K.D., 1994. Evolution of early Cenozoic marine temperatures. Paleoceanography 9, 353–387.

Zachos, J.C., Quinn, T.M., Salamy, K.A., 1996. High-resolution (104 years) deep-sea foraminiferal stable isotope record of the Eocene–Oligocene climate transition. Paleoceanography 11, 251–266.

Zachos, J.C., Shackleton, N.J., Revenaugh, J.S., Palike, H., Flower, B.P., 2001. Climate response to orbital forcing across the Oligocene–Miocene boundary. Science 292, 274–278.